

## Defects in N<sup>+</sup> ion-implanted ZnO single crystals studied by positron annihilation and Hall effect

G. Brauer<sup>\*,1</sup>, W. Anwand<sup>1</sup>, W. Skorupa<sup>1</sup>, J. Kuriplach<sup>2</sup>, O. Melikhova<sup>2</sup>, J. Cizek<sup>2</sup>, I. Prochazka<sup>2</sup>, H. von Wenckstern<sup>3</sup>, M. Brandt<sup>3</sup>, M. Lorenz<sup>3</sup>, and M. Grundmann<sup>3</sup>

<sup>1</sup> Institut für Ionenstrahlphysik und Materialforschung, Forschungszentrum Rossendorf, Postfach 510119, 01314 Dresden, Germany

<sup>2</sup> Department of Low Temperature Physics, Faculty of Mathematics and Physics, Charles University, V. Holesovickach 2, 180 00 Prague, Czech Republic

<sup>3</sup> Institut für Experimentelle Physik II, Universität Leipzig, Linnéstr. 5, 04103 Leipzig, Germany

Received 23 July 2006, accepted 5 March 2007

Published online 29 June 2007

PACS 61.72.Ji, 61.72.Vv, 72.20.My, 78.70.Bj

High quality ZnO single crystals of dimensions 10 x 10 x 0.5 mm<sup>3</sup>, grown by a hydrothermal approach, have been implanted by 40 keV N<sup>+</sup> ions to a fluence of 1 x 10<sup>15</sup> cm<sup>-2</sup> at room temperature. Their properties revealed by positron annihilation and Hall effect measurements are given in the as-grown and as-irradiated states, and after post-implantation annealing in an oxygen ambient at 200 °C and 500 °C.

© 2007 WILEY-VCH Verlag GmbH & Co. KGaA, Weinheim

**1 Introduction** Future applications of zinc oxide (ZnO), e.g. for visible and UV light emitters and detectors, will not only rely on provision of high-quality bulk material and films but on a full understanding of the role of lattice defects, as they largely control the optical and electrical properties [1, 2].

Positron Annihilation Spectroscopy (PAS) [3, 4], especially in the form of Slow Positron Implantation Spectroscopy (SPIS) using mono-energetic positrons [5, 6], is now a well-established tool for the study of electronic and defect properties of bulk solids and thin films.

Recently, a consistent theoretical modelling of bulk and defect positron properties of ZnO has been performed [7]. A survey of positron lifetimes in ZnO from the literature led to the conclusion that four well-separated lifetime levels exist between those for the bulk and the Zn vacancy – and it was postulated that a hydrogen-defect interaction could be responsible for this finding [8].

In the present study, hydrothermally grown ZnO single crystals are investigated by PAS and temperature-dependent Hall (TDH) measurements before and after implantation by 40 keV N<sup>+</sup> ions to a fluence of 1 x 10<sup>15</sup> cm<sup>-2</sup> at room temperature (RT), and post-implantation annealing.

**2 Experimental** Hydrothermally grown (HTG) high quality ZnO single crystals, of dimensions 10 x 10 x 0.5 mm, were supplied by MaTecK GmbH (Jülich) with the O-face polished.

PAS studies were performed by positron lifetime (PL) measurements using a fast-fast PL spectrometer with a timing resolution of 160 ps [9] collecting up to 10<sup>7</sup> events per spectrum. SPIS studies were performed with a positron energy adjustable from 0.03 to 36 keV accumulating about 10<sup>6</sup> events per spectrum [10]. The energy resolution of the Ge detector used is (1.09 ± 0.01) keV at 511 keV.

The motion of the electron-positron pair prior to annihilation causes a Doppler broadening of the 511 keV annihilation line and can be characterized by the line-shape parameters *S* and *W* [3, 4]. The depth

\* Corresponding author: e-mail: g.brauer@fz-rossendorf.de, Phone: +49 351 260 2117, Fax: +49 351 260 3285

information was obtained from the correlation of  $S$  and  $W$  with positron energy  $E$  using the versatile program package VEPFIT [11], in which a density of  $5.605 \text{ g cm}^{-3}$  for ZnO was used.

TDH measurements were performed in the temperature range 20–325 K at Leipzig using an automated Hall setup as in previous investigations [7].

After the PL and SPIS measurements were finished, the polished side (O-face) of the as-received ZnO single crystal was implanted at Rossendorf with  $\text{N}^+$  ions of 40 keV to a fluence  $1 \times 10^{15} \text{ cm}^{-2}$  at RT at an angle of  $7^\circ$  with respect to the surface normal in order to avoid ion channeling. Subsequent sample annealing at 200 °C and 500 °C was performed in an oxygen atmosphere.

**3 Results and discussion** The HTG ZnO samples investigated here are found to exhibit a single component positron lifetime spectrum with a lifetime of  $(182.1 \pm 0.4)$  ps. On the one hand, this is longer than the calculated ZnO bulk lifetime of 159 ps [7] as well as the ZnO bulk lifetime of  $(151 \pm 2)$  ps obtained from application of the two-state positron trapping model to the experimental PL data measured on a pressurized melt growth ZnO single crystal [7]. On the other hand, the lifetime is shorter than  $(214.2 \pm 0.6)$  ps reported for a negatively charged Zn-vacancy [8]. Thus, all positrons are trapped in a defect exhibiting an obviously smaller open volume than the Zn vacancy [7, 8]. The decrease of the positron lifetime, compared to that for a Zn vacancy in ZnO, could be due to the ‘attachment of hydrogen’ – an effect known to exist in metals [12] – but this needs further investigation and clarification.

The theoretical calculation of positron lifetimes for defects decorated with an impurity is a difficult task. In the case of HTG ZnO the decorating impurity of a Zn vacancy is most probably hydrogen. Hydrogen as a cause of doping has been extensively considered in a recent paper [13]. A very first and still rough calculation using the atomic superposition (ATSUP) method [14] has already been performed for two extreme cases: (a) the H atom is placed directly into the centre of the Zn vacancy, and (b) the H atom occupies a so-called perpendicular bond-centre position [13], and the results are: (a)  $\tau_{\text{defect}} = 185$  ps, (b)  $\tau_{\text{defect}} = 207$  ps [8]. The electron-positron correlation was treated using the corrected Boronski-Nieminen (BN) approach in the same way as in Ref. [7].

In the present work, these calculations have been refined by relaxing the geometry of the zinc vacancy plus the hydrogen defect using the Vienna ab initio simulation package (VASP; version 4.6.21) [15] and employing the local density approximation ultrasoft pseudopotentials [16] supplied along with the package. Positron calculations were carried out by means of the ATSUP method [14], using the relaxed defect configurations. It is found that H in a Zn vacancy stays close to one of neighbouring oxygen atoms, i.e. not in the vacancy centre, so that the free volume is reduced compared to the case when no H is present. The resulting lifetime (BN approach) amounts to 185 ps for the one possible configuration considered to date. The coincidence with the result for the non-relaxed defect mentioned above is just accidental as during the relaxation surrounding O atoms move mostly outward (relative to the vacancy centre) and the H atom moves to one of the surrounding oxygen atoms.

To estimate the extent of the subsurface region expected to be damaged due to the ion implantation performed, the profiles of ions and vacancies were simulated by TRIM [17] code calculations which show that the maxima of the vacancy and ion distributions are at depths of  $\sim 42$  and  $\sim 72$  nm, respectively.

In Fig. 1 SPIS results are presented. By VEPFIT [11] analysis it is found that the as-grown material exhibits a positron diffusion length  $L_+ = (22 + 1)$  nm [18]. This shows that the ion implantation creates open volume defects of yet unknown structure which must be more attractive to positrons than the defects already existing in the virgin sample. Neither fitting of a box-shaped (two layer model) nor a Gaussian defect profile is possible, which suggests that the real defect profile deviates considerably from both model profiles. However, from an estimate of the ratio  $S_{\text{impl}}(E)/S_{\text{virgin}}(E)$  it can be concluded that (i) a damaged layer is created that extends from  $\sim 10$  nm to  $\sim 170$  nm, and (ii) a narrow subsurface layer extending to a depth of  $\sim 10$  nm still exists that should be nearly free of ion implantation-induced defects. After annealing at 200 °C an increase of the surface  $S$  value is observed that indicates a slight surface and near-surface change of the sample, whereas the deeper defect profile remains unchanged. Due to the annealing at 500 °C two effects are visible: (i) the surface  $S$  value decreases compared to the previous

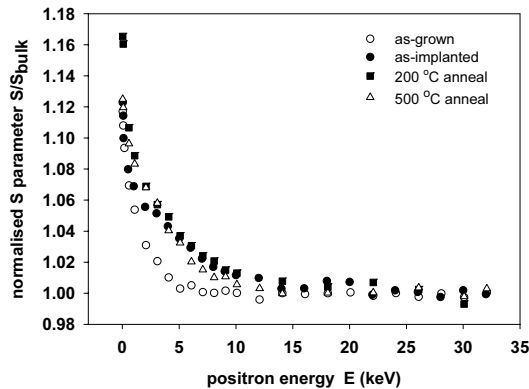


**Fig. 1** Doppler broadening parameter  $S$  of a ZnO single crystal in as-grown, as-implanted, and two annealed states, respectively, as a function of incident positron energy  $E$ .

sample treatment, and (ii) the implantation-induced defects begin to anneal out seen by the  $S(E)$  curve which is approaching the as-grown one.

Due to incorporation of group I elements (especially Li and Na), HTG ZnO single crystals are highly compensated - which means of very high electrical resistivity. At temperatures  $< \sim 180$  K, such semi-insulating samples become insulating and thus inaccessible to Hall effect measurements. Since scattering at ionized impurities is dominant for even lower temperatures, the density of compensating acceptors  $N_a$  cannot be determined reliably by fitting the Hall mobility. However, RT Hall mobility  $\mu_{RT}$  is an indirect measure of  $N_a$  - i.e. the lower  $\mu_{RT}$ , the higher  $N_a$ . The highest  $\mu_{RT}$  of  $\sim 160$  cm<sup>2</sup>/Vs is observed for the as-grown sample. It drops due to implantation to  $\sim 140$  cm<sup>2</sup>/Vs and increases again slightly to  $\sim 145$  cm<sup>2</sup>/Vs after annealing at 200 °C. Figure 2 shows the temperature dependence of the free carrier concentration  $n$  for different sample states. The large scatter of data points for the as-implanted sample below 200 K is due to the further rapid increase of sample resistivity with decreasing temperature. After annealing at 500 °C the resistivity of the sample becomes too high for temperature dependent measurements. The value of  $n$  is reduced by implantation and furthermore with each annealing step. However, the thermal activation energy which is represented by the slope of the drawn lines does not change (see Fig. 2).

Because Hall measurements give an integral value, one would expect to measure only small changes after implantation, since the implanted volume is small compared to the non-implanted volume of the sample. But the effect of implantation is clearly visible in Fig. 3, suggesting that the changes in the near surface region are drastic.

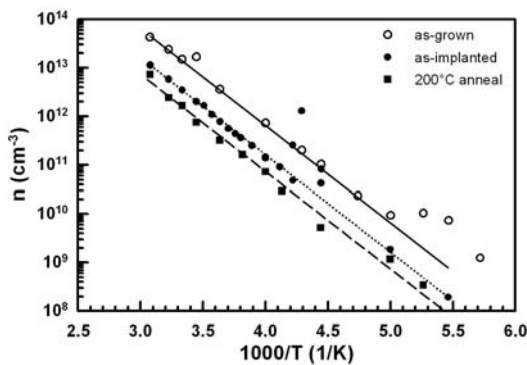


**Fig. 2** Free electron concentration  $n$  of a ZnO single crystal in various states as a function of reciprocal temperature  $1/T$ .

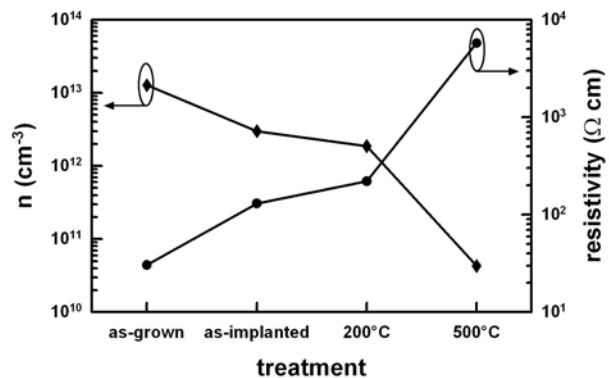


**Fig. 3** RT resistivity and free electron concentration  $n$  of a ZnO single crystal in various states.

Annealing at 200 °C leads to minor changes of the electrical properties. However, a large change is found after annealing at 500 °C. The value of  $n$  drops by a factor of 50 from  $\sim 2 \times 10^{12} \text{ cm}^{-3}$  to  $\sim 4 \times 10^{10} \text{ cm}^{-3}$ . It has recently been shown [7, 19] that this annealing stage ( $\sim 500$  °C in an oxygen ambient) is very effective for activating nitrogen acceptors and for reducing donor-like defects caused by ion implantation. Nevertheless, the HTG ZnO sample investigated here remains  $n$ -type.

**4 Conclusions** Results of refined calculations of the positron lifetime in a Zn vacancy decorated by one H atom are presented. Certainly, further improvements of these calculations - including more than one hydrogen atom - are required and remain a challenge for future work.

The formation of ion implantation-induced open-volume defects is clearly detected and its depth range characterized by SPIS measurements, and the electrical behaviour of the ZnO single crystal is clearly monitored by Hall measurements. The annealing behaviour is investigated up to 500 °C.

**Acknowledgements** Support of HvW by Deutsche Forschungsgemeinschaft (DFG) in the frame of grant Gr1011/10-2 (within SPP1136) is gratefully acknowledged. This work is part of the research plan MS 0021620834 that is financed by the Ministry of Education of the Czech Republic.

## References

- [1] D. S. Ginley and C. Bright (eds.), Mater. Res. Soc. Bull. **25**, 15 (2000).
- [2] D. C. Look, Mater. Sci. Eng. B **80**, 383 (2001).
- [3] A. Dupasquier and A. P. Mills, Jr. (eds.), Positron Spectroscopy of Solids (IOS, Amsterdam, 1995).
- [4] R. Krause-Rehberg and H. S. Leipner, Positron Annihilation in Semiconductors – Defect Studies (Springer, Berlin, 1999).
- [5] G. Brauer and W. Anwand (eds.), Slow Positron Beam Techniques for Solids and Surfaces, Appl. Surf. Sci. **194**, (2002).
- [6] I. Y. Al-Qaradawi and P. G. Coleman (eds.), Slow Positron Beam Techniques for Solids and Surfaces, Appl. Surf. Sci. **252** (2006).
- [7] G. Brauer, W. Anwand, W. Skorupa, J. Kuriplach, O. Melikhova, C. Moisson, H. von Wenckstern, H. Schmidt, M. Lorenz, and M. Grundmann, Phys. Rev. B **74**, 045208 (2006).
- [8] G. Brauer, J. Kuriplach, J. Cizek, W. Anwand, O. Melikhova, I. Prochazka, and W. Skorupa, Vacuum (2007), in print.
- [9] F. Becvar, J. Cizek, L. Lestak, I. Novotny, I. Prochazka, and F. Sebesta, Nucl. Instrum. Methods A **443**, 557 (2000).
- [10] W. Anwand, H.-R. Kissener, and G. Brauer, Acta Phys. Polon. A **88**, 7 (1995).
- [11] A. vanVeen, H. Schut, J. de Vries, R. A. Hakvoort, and M. R. Ijpma, in: Positron Beams for Solids and Surfaces, edited by P. J. Schultz, G. R. Massoumi, and P. J. Simpson (AIP, New York, 1990), p. 171.
- [12] J. Cizek, I. Prochazka, F. Becvar, R. Kuzel, M. Cieslar, G. Brauer, W. Anwand, R. Kirchheim, and A. Pundt, Phys. Rev. B **69**, 224106 (2004).
- [13] C. G. Van de Walle, Phys. Rev. Lett. **85**, 1012 (2000).
- [14] M. Puska and R. Nieminen, J. Phys. F: Met. Phys. **13**, 333 (1983).
- [15] G. Kresse and J. Hafner, Phys. Rev. B **47**, 558 (1993); Phys. Rev. B **49**, 14251 (1994); G. Kresse and J. Furthmüller, Comput. Mater. Sci. **6**, 15 (1996); G. Kresse and J. Furthmüller, Phys. Rev. B **54**, 11169 (1996).
- [16] G. Kresse and J. Hafner, J. Phys.: Condens. Matter **6**, 8245 (1994).
- [17] J. F. Ziegler, J. P. Biersack, and U. Littmark, The Stopping and Range of Ions in Solids (Pergamon, New York, 1985).
- [18] G. Brauer, W. Anwand, W. Skorupa, J. Kuriplach, O. Melikhova, J. Cizek, I. Prochazka, C. Moisson, H. von Wenckstern, H. Schmidt, M. Lorenz, and M. Grundmann, Superlattices Microstruct. (2006, submitted).
- [19] H. von Wenckstern, R. Pickenhain, H. Schmidt, M. Brandt, G. Biehne, M. Lorenz, M. Grundmann, and G. Brauer, Appl. Phys. Lett. **89**, 092122 (2006).